Effects of Intercrystal Crosstalk on Multielement LSO/APD PET Detectors

Paul Vaska, *Member, IEEE*, Sean P. Stoll, Craig. L. Woody, *Member, IEEE*, David J. Schlyer, and Sepideh Shokouhi

***Abstract*—One of the most promising high resolution positron emission tomography detector designs comprises an array of small, optically isolated scintillator crystals each coupled to an independent photosensor, such as an avalanche photodiode (APD). However, crosstalk between crystals (due to Compton scatter, photoelectron escape, or incomplete optical isolation) can significantly degrade performance and is expected to increase as crystals become narrower to improve spatial resolution. Various measures of crosstalk have been determined for different configurations of 4×8 blocks of 2 mm $\times$ 2 mm lutetium oxyorthosilicate (LSO) crystals coupled to matched Hamamatsu APD arrays. Results indicate that ignoring crosstalk signals could lead to a $\sim$ 30% loss in coincidence sensitivity for a tomograph using these detectors and a decrease in energy resolution of $\sim$ 2 percentage points. Spatial and time resolution would not be significantly affected with most practical front-end architectures.**

***Index Terms*—Biomedical nuclear imaging, gamma-ray detectors, optical crosstalk, positron emission tomography (PET), scintillation detectors.**

I. Introduction

ONE OF THE most promising high resolution positron emission tomography (PET) detector designs comprises an array of small optically isolated scintillator crystals each coupled to an independent photosensor, such as an avalanche photodiode (APD) [1]–[3] or one channel of a multichannel photomultiplier tube (MC-PMT) [4]. Examples of these components are shown in Fig. 1. Current commercial block detectors, on the other hand, typically utilize a multiplexed readout scheme which relies on light-sharing among a small number of photomultiplier tube (PMT) channels. However, this produces overlapping peaks in a position histogram of the block, limiting the potential spatial resolution [5]. Another disadvantage compared to the independent-readout block detector is increased pulse pileup at high count rates. A particular advantage of APDs is their extremely compact size which opens up new potential PET applications such as a miniaturized tomograph for brain studies in conscious rodents [6].

However, a new issue arises with independent-readout crystal arrays: how to handle crosstalk between crystals, defined here as when a single incident gamma ray causes signals in more than one readout channel. Crosstalk can reduce spatial, energy, and time resolution, all of which are important for PET. It arises from Compton scattering from one crystal to another [7], [8] or possibly the escape of the photoelectron from the primary crystal following photoelectric absorption. In addition, for practical reasons, optical isolation of the scintillation photons within a single crystal is never absolute. Each of these effects can be expected to increase as crystal size is reduced in an effort to achieve higher spatial resolution [9].

The degree of crosstalk has particularly important implications for the design of the front-end electronics to read out these blocks. If all of the gamma-ray signal can be contained within one crystal, theoretically there is no need for energy digitization since an energy window can be enforced via simple discriminator thresholds for each crystal. This would be highly desirable as it would help offset the added complexity and power consumption introduced by the large number of electronics channels required (one per crystal). On the other hand, if crosstalk is significant, the signals from neighboring crystals might need to be accounted for, requiring an energy-measuring ADC for each crystal.

In order to evaluate the practical effects of crosstalk, a method to correct for it should be defined, so that detector performance with and without the correction can be compared. In this work, the general definition of crosstalk correction is the use of the additional signals from crystals near the crystal of interaction to improve the detector performance. The most straightforward specific way to correct for crosstalk is to attempt to recover, or reconstruct, the true incident gamma-ray energy by summing signals from all crystals adjacent to the crystal of interaction. The crystal of interaction can be defined as the crystal with maximum signal, which is a good approximation in terms of the resulting spatial resolution [8]. This is the crosstalk correction approach used in this work. Including more crystals than adjacent nearest neighbors in the sum is unlikely to be an improvement since crosstalk is mostly a local effect and the distant crystals not involved in the event would mostly add noise to the summed signal, thus potentially having a net negative effect on energy resolution.

One benefit of this crosstalk correction method would be increased photopeak event acceptance, or sensitivity. For example, if a gamma-ray undergoes Compton scatter in one crystal and is then absorbed in its neighbor, the signal from each crystal might fall below its energy window, but the summed signal would be within the photopeak window, resulting in the acceptance of a useful event. Thus, one way to evaluate the tradeoffs between electronics architectures with and without ADCs is in terms of sensitivity. Assuming a constant energy window for the events (which implies a similar rejection of object scatter), the photopeak event acceptance rate of a crystal should be higher when

Manuscript received December 2, 2002. This work was supported by the U.S. Department of Energy (OBER) under Prime Contract DE-AC02-98CH10886.

The authors are with Brookhaven National Laboratory, Upton, NY 11973 USA (e-mail: vaska@bnl.gov).

Digital Object Identifier 10.1109/TNS.2003.812452

events are reconstructed this way using energy digitization compared to the simple per-crystal threshold case because crosstalk events may fall below the energy window until they are reconstructed. The difference in sensitivity is one measure of the impact of crosstalk on this front-end design choice.

Other effects of crosstalk correction must also be addressed. With regard to energy resolution, summing will of course increase the photopeak signal, but also the noise levels, so the net effect must be evaluated. Spatial resolution, on the other hand, is not expected to be significantly affected unless crosstalk levels are unexpectedly large. Previous work [8] suggests that for this type of detector, incorporation of signals from neighboring crystals has a negligible effect on spatial resolution. Finally, time resolution would not be affected by implementing crosstalk correction. Timing would still be determined from a single channel only, because it is very sensitive to noise, and summing channels before the timing discriminator would almost certainly degrade the resolution.

II. Materials and Methods

The present work explores the consequences of intercrystal crosstalk using 4×8 arrays of lutetium oxyorthosilicate (LSO) crystals with 2 mm $\times$ 2 mm cross section. The LSO array is coupled via a thin UV-transparent silicone wafer to a geometrically matched 4×8 APD array (S8550 from Hamamatsu Photonics, Japan) [3], [6]. Two different crystal configurations were studied, as shown in Fig. 1.

The first type is from CTI, Inc.[1] The block is approximately 8.5 mm thick and has a diffuse surface finish. The crystals in this array are actually not completely independent. Starting from a solid block, cuts are made $\sim 90\%$ through, leaving $\sim 10\%$ unsegmented for mechanical integrity. The block is wrapped in teflon tape followed by a mirror foil, and the spaces between crystals filled with a reflective SiO_2 powder.

The other type of crystal array is manufactured by Proteus, Inc.[2] with a 10 mm thickness and specular surface finish. The reflector is radiant mirror film from 3 M.[3] The construction begins with a solid LSO block which is first cut parallel to the short side into eight approximately square slabs and polished to a specular finish. Reflector sheets are inserted between slabs and the block glued back together. Then the block is cut along the long dimension, polished, and reassembled with the remaining reflectors glued in. Note that this results in continuous reflector sheets in the long direction and small pieces in the short direction.

The APDs are operated at a bias voltage of $\sim$ 370 V, which produces a stable gain of $\sim$ 50. Each of the 32 anode signals are routed through a preamp and 70 ns shaping amplifier to a signal splitter. One output of the splitter is used for energy measurement, feeding directly into a LeCroy 4300 FERA/ECL charge-integrating ADC. The other output is used for triggering the data acquisition system; each channel is routed to a LeCroy 3420 CFD (40 ns delay, 0.33 fraction) whose outputs are ORd together and then required to be in coincidence with the same signal from the opposing block. For these measurements, the coincidence requirement serves only to eliminate the natural background activity from the LSO. The trigger initiates integration of all crystals whenever at least one crystal from each block exceeds its threshold of $\sim$ 200 keV. Control of the acquisition system is via KmaxNT software[4] running on a PC.

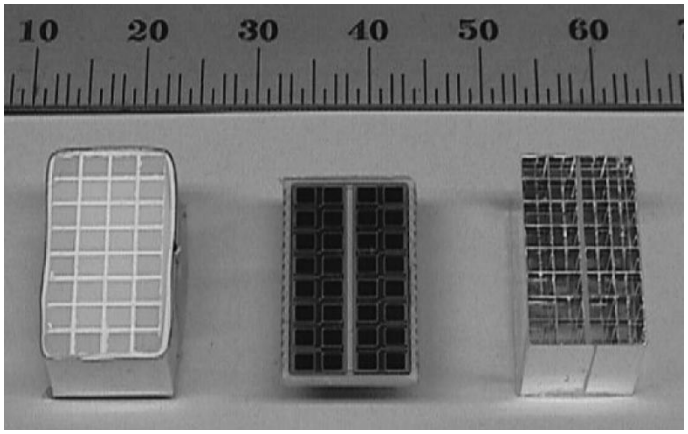

Fig. 1. CTI (left) and Proteus (right) LSO arrays with matching Hamamatsu S8550 APD array (center).

A 1.5 μCi ^{22}Na point source was centered between two identical blocks $\sim$ 6 cm apart and more than 300 000 coincidence events were collected. The listmode event stream was processed offline using two different schemes simulating system architectures with and without energy digitization. Both schemes produce an energy spectrum for each crystal by incrementing, for each event, only the spectrum of the crystal with the highest signal in the block.

The first scheme uses no crosstalk correction, which represents the case if energy digitization were not available. The energy spectrum for each crystal uses only the data from that crystal. Each spectrum was analyzed for centroid of the photopeak, percentage full-width at half-maximum (FWHM) resolution, and counts within a 400–700 keV energy window. The photopeak position for each crystal was used to create a set of gain-matching factors which were applied when processing the data in the second scheme.

The second scheme takes advantage of the energy digitization by summing the signals from adjacent channels to recover crosstalk events which may have fallen below the per-element energy window. The same event stream was processed again to create another energy spectrum for each channel, this time using the sum of (gain-matched) signals from all neighboring crystals to reconstruct the total event energy (4–9 crystals in each sum depending on location in the block). Again, the FWHM energy resolution and counts in the same 400–700 keV window were recorded. In addition, the signal-weighted position centroid of each event was incremented into a two-dimensional "flood" histogram to observe the effect of crosstalk on a centroid positioning scheme.

An additional measurement was made of the absolute light output of the individual CTI and Proteus crystals (with

[1]Knoxville, TN, USA.

[2]Chagrin Falls, OH, USA.

[3]St. Paul, MN, USA.

[4]Sparrow Corp., Starkville, MS, USA.

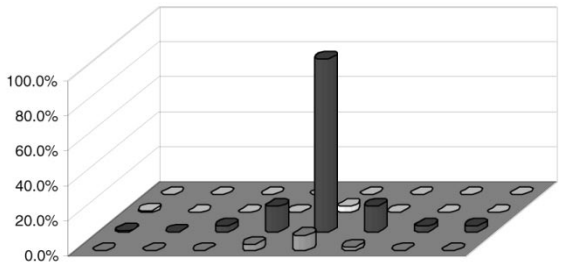

Fig. 2. Distribution of crosstalk signals for a selected crystal in the Proteus array.

TABLE I
MEASURED PROPERTIES OF CTI AND PROTEUS BLOCKS

Property	Array CTI	Proteus
cross-talk (increase in signal magnitude after correction) (%)	20.7	35.6
increase in coincidence sensitivity after correction (%)	33.7	25.1
FWHM energy resolution (%, before/after correction)	22.0/20.0	17.2/18.1
light output (primary APD photoelectrons/MeV)	3020	1750

no crosstalk correction). This was done by measuring the photopeak positions for each crystal using the same APD and electronics setup for each block. These values were first converted to the number of electrons at the input to the electronics using calibration factors determined from the injection of a known charge into each channel. This was then converted to the number of primary photoelectrons in the APD by dividing by the measured APD gain.

III. RESULTS

Fig. 2 depicts the distribution of crosstalk signals for a selected crystal in the Proteus array. A quantitative measure of crosstalk is the increase in signal produced by crosstalk correction (the inclusion of signals from adjacent crystals). The average increase in the photopeak position for the two blocks is shown in the first row of Table I.

An example of the effect on the energy spectrum of a selected crystal from the CTI block is shown in Fig. 3. The spectrum with correction (dashed) has been compressed to align the peaks so that the resolution and sensitivity can be directly compared. Note the larger number of counts above threshold and the improved resolution at FWHM in the corrected case. The average energy resolutions before and after crosstalk correction are shown in the third row of Table I. The CTI array shows an improvement with crosstalk correction, while the Proteus block degrades slightly.

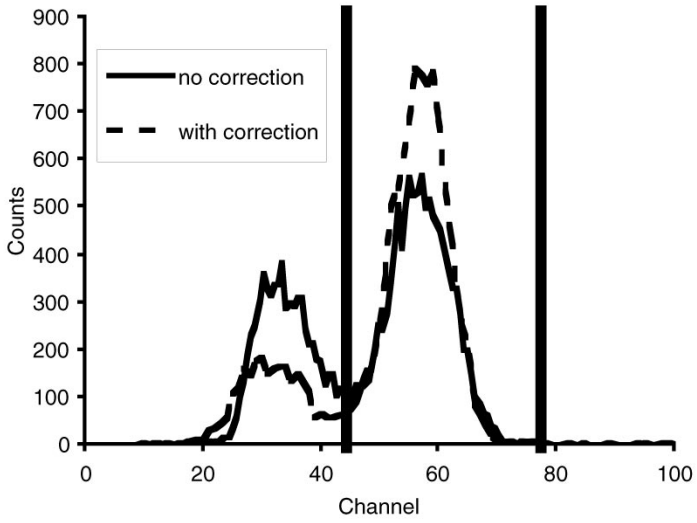

Fig. 3. Energy spectra of crystal from CTI block with (dashed line) and without (solid line) crosstalk correction, scaled to the same peak position. Vertical lines indicate the 400–700 keV energy window.

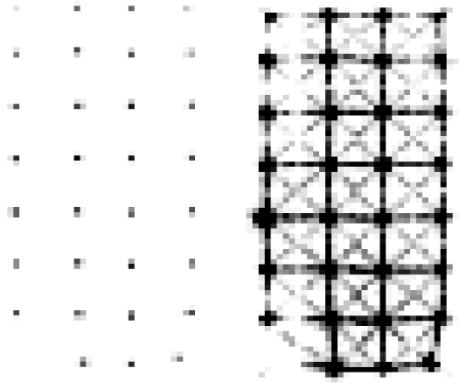

Fig. 4. Flood histogram of CTI detector using signals from adjacent crystals in a centroid positioning method. The left image is scaled to the maximum pixel, and the right image is purposely saturated to show the weak structures between pixels.

The second row of Table I shows the predicted increase in coincidence sensitivity as a result of crosstalk correction. It is the square of the average sensitivity increase from one block. The CTI block has somewhat more to gain from crosstalk correction than does the Proteus block. The last row shows that the CTI block has $\sim$ 1.7 times the light output of the Proteus block.

Fig. 4 is a "flood" histogram of event positions for the CTI block detector using a simple signal-weighted centroid positioning scheme of nearest neighbors. The image on the right has an oversaturated gray scale to reveal the weak structures between crystals, at less than 3% of the peak intensities. Fig. 5 is the same except that the block is exposed to gamma-rays from the right side.

IV. DISCUSSION

The similar thickness of the CTI and Proteus blocks implies a similar contribution to the crosstalk from gamma-ray and

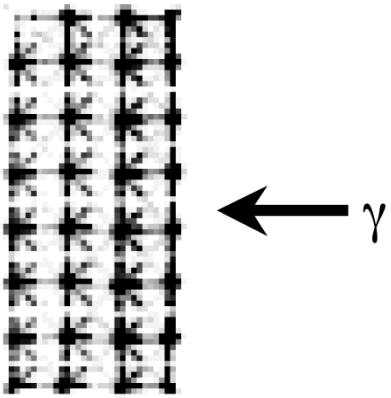

Fig. 5. Flood histogram of Proteus block exposed to 511-keV photons from the right side, with maximum of gray scale reduced to show intercrystal structures.

photoelectron scattering. This is because these effects are only a function of the type of scintillator and its geometry. Thus the larger crosstalk in the Proteus block from Table I is most likely optical in origin, i.e., due to the escape of scintillation photons from the primary crystal. This is supported by the distribution of crosstalk in the Proteus block, shown in Fig. 2, in that there is less crosstalk between crystals separated by a continuous reflector sheet (along the long axis), than between crystals separated by the narrow, cut reflector strips running along the short axis.

At first glance, the measurements might seem contradictory. The Proteus array has more crosstalk on average, but less to gain from the correction in terms of sensitivity or resolution. The CTI block has much higher light output, but lower energy resolution. However, a consistent explanation can be made as follows.

The first observation is that the high light output and poorer energy resolution of the CTI block strongly suggests that the resolution is not dominated by photoelectron statistics. A rough estimate of the contribution from statistical noise is the reciprocal of the square root of the minimum number of charge carriers (photoelectrons in this case). Indeed, this would be only 6.0% FWHM for the CTI block and 7.9% for the Proteus block, a small difference in a quadrature sum equal to a total resolution of $\sim 20\%$.

Thus, based on the above observations, differences between the blocks are mostly optical, but not affected much by differences in average light output. This leaves few plausible explanations for the measured differences in energy resolution; the most obvious is that light collection efficiency varies depending on the location of the gamma-ray interaction. Similarly, the *change* in energy resolution of a given block due to crosstalk correction should have a similar cause. The CTI block showed a modest improvement in resolution with crosstalk correction, evidently because the correction reduced the position dependence of the total light output. This would be consistent with the CTI design which has a continuous (and thus optically leaky) portion at the gamma-ray entrance surface. On the other hand, the lack of improvement from crosstalk correction in the Proteus block suggests that the added signal does not improve the position dependence, or conversely, that the light leakage is not dependent on the interaction location. The observed slight degradation in resolution might be due to the added noise from summing multiple electronics channels.

A similar argument can be made for the sensitivity. Since differences between the blocks are mostly optical, the larger improvement in sensitivity from the crosstalk correction in the CTI block implies that the correction is recovering more events from locations which produce relatively low light output in the crystal of interaction. Again, these locations are likely near the continuous front face.

The flood histograms of Figs. 4 and 5 also provide information about the crosstalk. While the peak corresponding to a given crystal is slightly blurred, there is very little overlap between crystals, suggesting a negligible difference in spatial resolution between the two schemes, as expected. More complicated crosstalk correction schemes which might improve spatial resolution have been proposed, such as those which attempt to correctly position Compton-scattered events at the crystal-of-first-interaction by modeling the Compton kinematics [10], [11]. However, optical crosstalk must be carefully modeled, and in any case, simulations [8] suggest that there is not much room for improvement in this regard.

In the saturated grayscale images, note the weak "connect-the-dot" ridge structures which appear at less than 3% of the intensity of the peaks and have been observed earlier with a similar detector which uses a position-sensitive PMT instead of APDs [12]. They are consistent with Compton scatter or photoelectron penetration between adjacent crystals, because a ridge is formed when only two neighboring crystals have significant signals in an event, and the ratios of the two signals varies from event to event. While optical crosstalk might produce some structure between specific neighbors (due to an imperfect reflector between them, for example) it is difficult to imagine how it would produce such a symmetric pattern with all neighbors.

Furthermore, Fig. 5 suggests that these events are largely Compton scatter. The gamma rays are moving to the left in the figure, and the ridge structures appear to extend mainly to the right of the crystal centers. This is consistent with Compton scatter in which the scattered gamma ray preferentially scatters in the direction of the incident gamma ray, depositing a relatively smaller amount of energy in the crystal of first interaction. If the scattered gamma ray is then absorbed in an adjacent crystal (preferentially to the left), the event will be positioned closer to the second (left) crystal because a larger fraction of the energy is deposited there. Hence, a ridge extending to the right of a crystal center in reality mostly contains events which first interacted in a crystal to the right, specifically the one pointed to by the ridge. This is a demonstration of the effect modeled by the Compton kinematic algorithms mentioned above.

V. Conclusion

The results indicate that crosstalk has a measurable impact on the performance of these detector blocks and suggests that crosstalk correction (which requires energy digitization for each crystal) would provide a significant benefit in sensitivity and potentially energy resolution as well. Spatial resolution would

be similar for the two schemes, although more sophisticated methods might improve it somewhat.

Although the Proteus design is not as light-tight on the average as the CTI design, the degree of crosstalk is less dependent on event position resulting in better energy resolution and less need for crosstalk correction approaches. Depending on the constraints of the electronics design for a particular application, the sensitivity loss from forgoing a system design with crosstalk correction may be tolerable. The lower average light output of the Proteus block, however, may limit the achievable time resolution and places higher demands on noise performance in the readout electronics.

ACKNOWLEDGMENT

The authors are grateful for the electronics expertise provided by the personnel of the Brookhaven Instrumentation Division.

REFERENCES

[1] R. Lecomte, C. Martel, and J. Cadorette, "Study of the resolution performance of an array of discrete detectors with independent readouts for positron emission tomography," *IEEE Trans. Med. Imag.*, vol. 10, pp. 347–357, 1991.

[2] Y. Shao, R. W. Silverman, R. Farrell, L. Cirignano, R. Grazioso, K. S. Shah, G. Vissel, M. Clajus, T. O. Tumer, and S. R. Cherry, "Design studies of a high resolution PET detector using APD arrays," *IEEE Trans. Nucl. Sci.*, vol. 47, pp. 1051–1057, 2000.

[3] B. J. Pichler, F. Bernecker, G. Boning, M. Rafecas, W. Pimpl, M. Schwaiger, E. Lorenz, and S. I. Ziegler, "A 32-Channel LSO matrix coupled to a monolithic 4×8 APD array for high resolution PET," *Proc. 2000 IEEE Medical Imaging Conf.*, 2000.

[4] S. R. Cherry, Y. Shao, S. Siegel, R. W. Silverman, E. Mumcuoglu, K. Meadors, and M. E. Phelps, "Optical fiber readout of scintillator arrays using a multi-channel PMT: A high resolution PET detector for animal imaging," *IEEE Trans. Nucl. Sci.*, vol. 43, pp. 1932–1937, 1996.

[5] Y. C. Tai, A. Chatziioannou, S. Siegel, J. Young, D. Newport, R. N. Goble, R. E. Nutt, and S. R. Cherry, "Performance evaluation of the microPET P4: A PET system dedicated to animal imaging," *Phys. Med. Biol.*, vol. 46, pp. 1845–1862, 2001.

[6] P. Vaska, D. J. Schlyer, C. L. Woody, S. P. Stoll, V. Radeka, and N. Volkow, "Imaging the unanesthetized rat brain with PET: A feasibility study," *2001 IEEE NSS/MIC Conf. Rec.*, vol. M9A-8, 2001.

[7] Y. Shao, S. R. Cherry, S. Siegel, and R. W. Silverman, "A study of inter-crystal scatter in small scintillator arrays designed for high resolution PET imaging," *IEEE Trans. Nucl. Sci.*, vol. 43, pp. 1938–1944, 1996.

[8] R. S. Miyaoka and T. K. Lewellen, "Effect of detector scatter on the decoding accuracy of a DOI detector module," *IEEE Trans. Nucl. Sci.*, vol. 47, pp. 1614–1619, 2000.

[9] A. Chatziioannou, Y. C. Tai, N. Doshi, and S. R. Cherry, "Detector development for microPET II: A 1 microliter resolution PET scanner for small animal imaging," *Phys. Med. Biol.*, vol. 46, pp. 2899–2910, 2001.

[10] M. Rafecas, G. Boning, B. J. Pichler, E. Lorenz, M. Schwaiger, and S. I. Ziegler, "Characterization and processing of inter-crystal scatter in a dual layer, high resolution LSO-APD–PET," *2001 IEEE NSS/MIC Conf. Rec.*, vol. M3–3, 2001.

[11] K. A. Comanor, P. R. G. Virador, and W. W. Moses, "Algorithms to identify detector Compton scatter in PET modules," *IEEE Trans. Nucl. Sci.*, vol. 43, pp. 2213–2218, 1996.

[12] J. J. Vaquero, J. Seidel, S. Siegel, W. R. Gandler, and M. V. Green, "Performance characteristics of a compact position-sensitive LSO detector module," *IEEE Trans. Med. Imag.*, vol. 17, pp. 967–978, 1998.